LAWRENCE
LIVERMORE
NATIONAL
LABORATORY

LLNL-JRNL-667121

Direct detection of Stealth Dark Matter through Electromagnetic Polarizability

T. Appelquist, E. Berkowitz, R. C. Brower, M. I. Buchoff, G. T. Fleming, X. Y. Jin, J. Kiskis, G. D. Kribs, M. F. Lin, E. T. Neil, J. C. Osborn, C. Rebbi, E. Rinaldi, D. Schaich, C. Schroeder, S. Syritsyn, P. Vranas, E. Weinberg, O. Witzel

February 10, 2015

Physical Review Letters

Disclaimer

This document was prepared as an account of work sponsored by an agency of the United States government. Neither the United States government nor Lawrence Livermore National Security, LLC, nor any of their employees makes any warranty, expressed or implied, or assumes any legal liability or responsibility for the accuracy, completeness, or usefulness of any information, apparatus, product, or process disclosed, or represents that its use would not infringe privately owned rights. Reference herein to any specific commercial product, process, or service by trade name, trademark, manufacturer, or otherwise does not necessarily constitute or imply its endorsement, recommendation, or favoring by the United States government or Lawrence Livermore National Security, LLC. The views and opinions of authors expressed herein do not necessarily state or reflect those of the United States government or Lawrence Livermore National Security, LLC, and shall not be used for advertising or product endorsement purposes.

The background field method is implemented following Refs. [34, 35] where the uniform background field is included by multiplying the unitary gauge links by two phase terms, chosen so that the field is oriented in the $\hat{z}$ direction. Quantization of the uniform background field on a torus restricts the available field strengths to values

$$\mathcal{E}/a^2 = \frac{2\pi e n}{|q_{\text{low}}| N_t N_s}, \tag{6}$$

where a is the lattice spacing, e is the electromagnetic coupling, N_s and N_t are the number of spatial and temporal lattice sites respectively, and q_{low} is the lowest common denominator of the charges (for SU(3), $q_{\text{low}} = 1/3$; for SU(4), $q_{\text{low}} = 1/2$).

For convenience we define a rescaled, dimensionless background field by $\tilde{\mathcal{E}} = (ea^2)^{-1}\mathcal{E}$. We will analyze our lattice results using Eqs. (4)-(5) with all quantities replaced with their rescaled, dimensionless counterparts, all of which will be denoted with a tilde:

$$m_B = \tilde{m}_B/a, \tag{7}$$

$$C_F = 4\pi\alpha a^3 \tilde{C}_F, \tag{8}$$

$$\mu_B = 4\pi\alpha\tilde{\mu}_B. \tag{9}$$

Lattice details and fitting – The lattice calculations are done using the *Chroma* software package [36]. We use the plaquette gauge action with unimproved Wilson fermions. The gauge configurations are quenched $N_s^3 \times N_t = 32^3 \times 64$ lattices (20000 heat-bath updates, 200 configurations separated evenly). For SU(4) we choose $\beta = 11.028$ and for SU(3) $\beta = 6.0175$ following [37]. Fermionic propagators are calculated for two different masses at each N_D value ($\kappa = 0.1554, 0.15625$ for $N_D = 4$ and $\kappa = 0.1537, 0.1547$ for $N_D = 3$), chosen such that the ratio of the pseudoscalar to vector meson masses $m_{PS}/m_V = 0.77$ and 0.70 are matched [14, 37].

Background field measurements are performed at six field values [$n = 0, ..., 5$, see Eq. (6)] for both $N_D = 4$ and $N_D = 3$, with correlation functions measured using 40 evenly separated sources in (x, y) along the $t = z = 0$ plane. Each zero and non-zero field value has 8000 measurements. All two-point correlation functions are fit over the range $t \in [4, 28]$ using fully correlated, multi-exponential fits including three excited states.

For $N_D = 4$, the two-point baryonic correlation function in background field $\tilde{\mathcal{E}}$ takes the form

$$C_B(t, \tilde{\mathcal{E}}) \sim Z(\tilde{\mathcal{E}}) \exp\left[-t\tilde{E}_B(\tilde{\mathcal{E}})\right] \tag{10}$$

at large t. Results for $\tilde{E}_B(\tilde{\mathcal{E}})$ are then fit to Eq. (4). We include higher-order contributions from the background field following [35],

$$\tilde{C}_F(\tilde{\mathcal{E}}) = \tilde{C}_F + \tilde{C}'_F|\tilde{\mathcal{E}}|^2. \tag{11}$$

The analysis for $N_D = 3$ is complicated by the contribution of the magnetic moment $\tilde{\mu}_B$ to the baryon self-energy. Following [35], we make use of the boost projections

$$\mathcal{P}_\pm = \frac{1}{2}\left(1 \pm i\gamma_3\gamma_4\right), \tag{12}$$

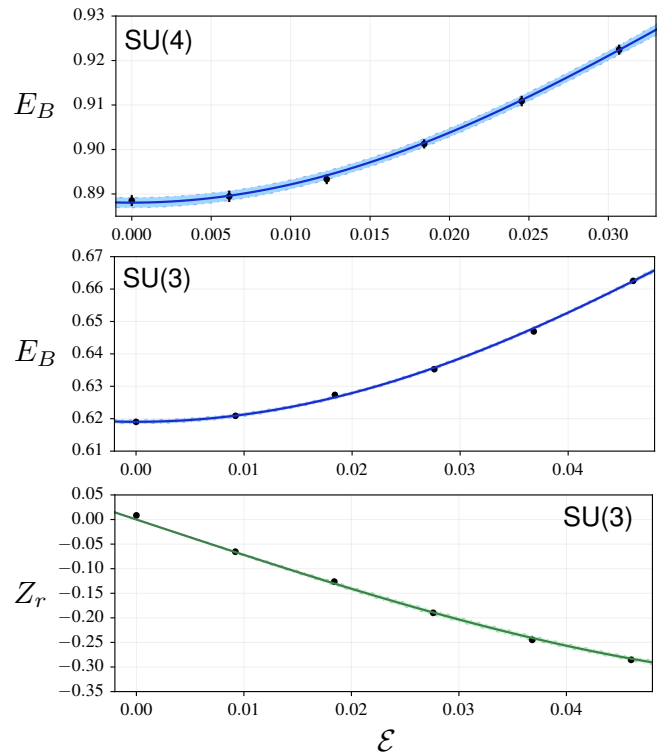

FIG. 1. The ground state energy (in lattice units) vs. applied electric field $\mathcal{E}$ for SU(4) baryons (top) and SU(3) baryons (middle), and ratio of projected SU(3) correlators vs. $\mathcal{E}$ (bottom). Their relations to the magnetic moment and polarizabilities are presented in Eqs. (4), (5) and (14). Results shown are for the ensembles with $m_{PS}/m_V = 0.70$.

and the boosted correlators

$$\begin{aligned} C_B^\pm(t) &= \langle \bar{B}(\mathbf{x}, t)\mathcal{P}_\pm B(\mathbf{0}, 0)\rangle_{\mathcal{E}} \\ &= Z_\pm(\tilde{\mathcal{E}}) \exp\left[-t\tilde{E}_B(\tilde{\mathcal{E}})\right]. \end{aligned} \tag{13}$$

The boost-projected amplitudes $Z_\pm$ contain equal and opposite contributions from the magnetic moment, which we isolate by combining them in the ratio

$$Z_r \equiv \frac{Z_+(\tilde{\mathcal{E}}) - Z_-(\tilde{\mathcal{E}})}{Z_+(\tilde{\mathcal{E}}) + Z_-(\tilde{\mathcal{E}})} = \frac{\tilde{\mathcal{E}}\tilde{\mu}_B(\tilde{\mathcal{E}})}{2\tilde{m}_B^2}. \tag{14}$$

A simultaneous fit of $\tilde{E}_B$ to Eq. (5) and the amplitude ratio in Eq. (14) allows us to determine both $\tilde{C}_F$ and $\tilde{\mu}_B$. To extract the polarizability $\tilde{C}_F$ we use a fully correlated quadratic fit following Eqs. (4)-(5). Once again we incorporate quadratic terms to both $\tilde{C}_F$ [as in Eq. (11)] and $\tilde{\mu}_B$,

$$\tilde{\mu}_B(\tilde{\mathcal{E}}) = \tilde{\mu}_B + \tilde{\mu}'_B|\tilde{\mathcal{E}}|^2. \tag{15}$$

The polarizability results for both SU(4) and SU(3) are presented in Table I, and results for the energies and the ratio Z_r vs. background field for the $m_{PS}/m_V = 0.70$ ensembles are plotted in Fig. 1.

N_D	m_{PS}/m_V	$\tilde{m}_B$	$\alpha\tilde{C}_F$	$\alpha^2\tilde{C}'_F$	$\tilde{\mu}_B$	$\tilde{\mu}'_B$	χ^2/dof
4	0.77	0.98204(93)	0.1420(56)	-0.089(29)	—	—	0.7/3
	0.70	0.88805(113)	0.1514(106)	-0.142(68)	—	—	4.8/3
3	0.77	0.69812(51)	0.2829(127)	-0.177(45)	-6.87(26)	714(103)	3.0/7
	0.70	0.61904(59)	0.2829(81)	-0.165(24)	-5.55(18)	396(78)	13.4/7

TABLE I. Results for the polarizabilities and magnetic moments of the baryonic composites of a strongly-coupled SU(N_D) theory, in lattice units.

Constructing the dimensionless product $\alpha\tilde{C}_F\tilde{m}_B^3$ (as needed for the DM cross section), we find that the SU(4) polarizabilities are larger than SU(3) by about 50%. Thus, we find the SU(3) and SU(4) polarizabilities to be comparable when normalized to the baryon mass. Of course, the baryon mass itself scales proportional to N_D; if we were to set the scale using a quantity such as the string tension which does not scale with N_D, then the SU(3) polarizability would be larger.

The effect of the quenched approximation, in which dynamical fermion loops are omitted from the lattice calculation, is not straightforward to estimate. However, the effects of such loops are expected to be suppressed with large N_D and heavy fermion mass; we note that even for QCD with its much lighter fermions, the effects of quenching are generally at most of order 10% [38].

Our calculations are performed at a single lattice spacing and volume, both of which can lead to additional systematic effects. We expect all of these corrections to be small relative to the order of magnitude uncertainty taken for the nuclear matrix element M_F^A. As a cross-check, we note that the neutron polarizability from the PDG [39] gives $C_F m_n^3 \simeq 0.36$ at the QCD physical ratio $m_{PS}/m_V = 0.18$, while our SU(3) lattice simulations give $C_F m_B^3 \simeq 0.84$ at $m_{PS}/m_V = 0.70$. These results are broadly consistent with the expected scaling of the polarizability and baryon mass with m_{PS}.

Direct detection cross sections – To relate the dimensionless lattice results to the dimensionful DM mass, m_B, that we vary continuously in order to scan the parameter space of the theory, it is most convenient to give units to the lattice spacing $a = \tilde{m}_B/m_B$. Along with Eq. (8), this leads to the physical value of the polarizability

$$C_F = 4\pi\alpha \left(\frac{\tilde{m}_B}{m_B}\right)^3 \tilde{C}_F \,. \tag{16}$$

Putting everything together, the spin-independent cross section written as the conventional *per nucleon* rate for a nucleus with (Z, A) from Eq. (2) becomes

$$\sigma_{\rm nucleon}(Z,A) = \frac{Z^4}{A^2}\frac{144\pi\alpha^2\mu_{nB}^2(M_F^A)^2}{m_B^6 R^2}[\alpha\tilde{m}_B^3\tilde{C}_F]^2 \,, \tag{17}$$

where we use our lattice results in Table I to evalate the factor in square brackets. We emphasize that, unlike Higgs exchange, the cross section *per nucleus* scales as Z^4 and not A^2, and so the cross section *per nucleon* must be calculated for each nucleus separately in order to compare with experiment. The strongest bound on the spin-independent direct detection scattering rate is from LUX [1]. In Fig. 2, we show the scattering cross section per nucleon for xenon, and compare with the LUX bounds. We plot only the $N_D = 4$ case here, as the $N_D = 3$ baryons are already excluded up to $\sim$ 20 TeV in mass by the LUX bounds through their magnetic moments [12].

Discussion – Our lattice results have allowed us to calculate the spin-independent scattering cross section of SU(4) stealth DM through polarizability, which we compare against the LUX constraints in Fig. 2. We find DM masses less than about 200 GeV are excluded, while the DM mass range 200-700 GeV could be probed by future experiments before reaching the neutrino background [40]. Currently, the strongest lower bound on the DM mass arises indirectly from the constraints on the lighter electrically-charged mesons that can be produced and decay promptly in collider experiments. Using our results [23], we estimate that DM masses below about 280 GeV are excluded given the LEP II bounds on the pseudoscalar mesons.

It is remarkable that a composite DM particle with a weak-scale mass, composed of dark fermions charged under the weak and electromagnetic interaction, can nevertheless be safe from both direct detection constraints and the LEP II constraint once $m_B \gtrsim 300$ GeV. This suggests there is a serious opportunity for future direct detection experiments to probe the model. Given that the scattering cross section per nucleon scales as $Z^4/(A^2R^2)$ in Eq. (17), the experiments with the heaviest nuclei are often more sensitive, i.e., xenon is 3.4 times more sensitive than argon if both experiments reach the same limit on the (conventional) spin-independent scattering per nucleon through Higgs exchange.

With our lattice calculation of the dark matter polarizability in this model, the dominant remaining uncertainty stems from the treatment of the non-perturbative nuclear matrix element in Eq. (2), which is similar to the matrix elements required for double beta decay. A significant source of uncertainty is, for example, the presence of excited states in Xe-129 and Ge-73 that have energies of 30 and 15 keV, which will be probed by the loop in the cross section calculation (typical momenta exchanges are roughly at the MeV scale). These resonances could appreciably change the resulting cross section, though the steep dependence on the dark matter mass suggests only a modest equivalent shift of the DM mass.

The brightest opportunity for stealth dark matter discovery may fall within the domain of the Large Hadron Collider (and future colliders). Meson phenomenology is very promising, since charged mesons can be produced through electroweak processes and decay completely into SM particles. In contrast, production of the dark matter baryon is rare, since it is considerably heavier than the mesons and

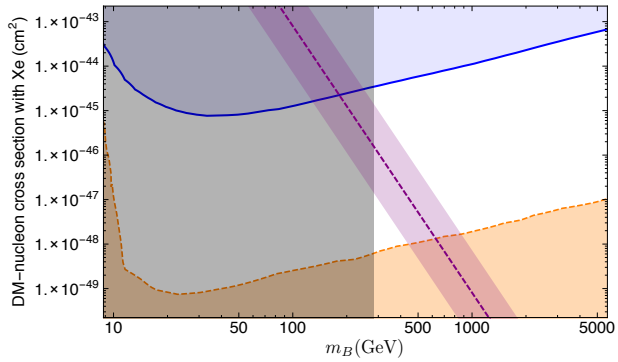

FIG. 2. The DM spin-independent scattering cross section per nucleon evaluated for xenon is shown as the purple band obtained from the SU(4) polarizability, where the width of the band corresponds to $1/3 < M_F^A < 3$ from low to high. The blue curve and the light blue region above it is excluded by the LUX constraints [1]. The vertical, darker shaded region is excluded by the LEP II bound on charged mesons [23]. The orange region represents the limit at which direct detection experiments will be unable to discriminate DM events from coherent neutrino recoil [40]. We emphasize that this plot is applicable for xenon, and would require calculating Eq. (17) to apply to other nuclei.

would have form factor suppression. This implies the standard missing energy signals that arise from DM production and escape from the detector are *rare*.

Finally, there are many avenues for further investigation of stealth dark matter, detailed in [23]. One vital issue is to better estimate the abundance. In the DM mass regime where stealth DM is detectable at direct detection experiments, the abundance of stealth dark matter can arise naturally from an asymmetric production mechanism [23] that was considered long ago [7–9] and more recently reviewed in [41]. If there is indeed an asymmetric abundance of bosonic dark matter, there are additional astrophysical consequences [42–44] that warrant further investigation to constrain or probe stealth DM.

Acknowledgements – MIB would like to thank Silas Beane, Paulo Bedaque, Tom Cohen, Jon Engel, Wick Haxton, David B. Kaplan, Jerry Miller, Maxim Pospelov, Sanjay Reddy, Martin Savage, Achim Schwenk, and Luca Vecchi for enlightening discussions on the full complexity of the nuclear physics calculation required for an accurate cross section prediction. We are also indebted to Brian Tiburzi for access to information that allowed for very useful checks of our background field code. We thank the Lawrence Livermore National Laboratory (LLNL) Multiprogrammatic and Institutional Computing program for Grand Challenge allocations and time on the LLNL BlueGene/Q (rzuseq and vulcan) supercomputer. We thank LLNL for funding from LDRD 13-ERD-023 "Illuminating the Dark Universe with PetaFlops Supercomputing". Computing support for this work was provided in part from the LLNL Institutional Computing Grand Challenge program and from the USQCD Collaboration, which is funded by the Office of Science of the US Department of Energy. MIB thanks the University of Oregon and University of Maryland, College Park for hospitality during the course of this work.

This work has been supported by the U. S. Department of Energy under Grant Nos. de-sc0008669 and de-sc0009998 (D.S.), de-sc0010025 (R.C.B., C.R., E.W.), DE-FG02-92ER-40704 (T.A.), de-sc0011640 (G.D.K.), DE-FG02-00ER41132 (M.I.B.), and Contracts DE-AC52-07NA27344 (LLNL), DE-AC02-06CH11357 (Argonne Leadership Computing Facility), and by the National Science Foundation under Grant Nos. NSF PHY11-00905 (G.F.), OCI-0749300 (O.W.). Brookhaven National Laboratory is supported by the U. S. Department of Energy under contract de-sc0012704. S.N.S was supported by the Office of Nuclear Physics in the U. S. Department of Energy's Office of Science under Contract DE-AC02-05CH11231.

* Present address: Higgs Centre for Theoretical Physics, School of Physics & Astronomy, The University of Edinburgh, EH9 3FD, UK

[1] D. Akerib *et al.* (LUX Collaboration), (2013), arXiv:1310.8214 [astro-ph.CO].
[2] R. Agnese *et al.* (SuperCDMS Collaboration), Phys.Rev.Lett. **112**, 241302 (2014), arXiv:1402.7137 [hep-ex].
[3] P. Cushman, C. Galbiati, D. McKinsey, H. Robertson, T. Tait, *et al.*, (2013), arXiv:1310.8327 [hep-ex].
[4] M. Xiao *et al.* (PandaX Collaboration), Sci.China Phys.Mech.Astron. **57**, 2024 (2014), arXiv:1408.5114 [hep-ex].
[5] S. Nussinov, Phys.Lett. **B165**, 55 (1985).
[6] R. S. Chivukula and T. P. Walker, Nucl.Phys. **B329**, 445 (1990).
[7] S. M. Barr, R. S. Chivukula, and E. Farhi, Phys.Lett. **B241**, 387 (1990).
[8] S. M. Barr, Phys.Rev. **D44**, 3062 (1991).
[9] D. B. Kaplan, Phys.Rev.Lett. **68**, 741 (1992).
[10] R. Lewis, C. Pica, and F. Sannino, Phys.Rev. **D85**, 014504 (2012), arXiv:1109.3513 [hep-ph].
[11] A. Hietanen, C. Pica, F. Sannino, and U. I. Sondergaard, Phys.Rev. **D87**, 034508 (2013), arXiv:1211.5021 [hep-lat].
[12] T. Appelquist, R. C. Brower, M. I. Buchoff, M. Cheng, S. D. Cohen, G. T. Fleming, J. Kiskis, M. F. Lin, E. T. Neil, J. C. Osborn, C. Rebbi, D. Schaich, C. Schroeder, S. N. Syritsyn, G. Voronov, P. Vranas, and J. Wasem (Lattice Strong Dynamics (LSD) Collaboration), Phys.Rev. **D88**, 014502 (2013), arXiv:1301.1693 [hep-ph].
[13] A. Hietanen, R. Lewis, C. Pica, and F. Sannino, JHEP **1412**, 130 (2014), arXiv:1308.4130 [hep-ph].
[14] T. Appelquist, E. Berkowitz, R. C. Brower, M. I. Buchoff, G. T. Fleming, J. Kiskis, G. D. Kribs, M. Lin, E. T. Neil, J. C. Osborn, C. Rebbi, E. Rinaldi, D. Schaich, C. Schroeder, S. Syritsyn, G. Voronov, P. Vranas, E. Weinberg, and O. Witzel (Lattice Strong Dynam-

ics (LSD) Collaboration), Phys.Rev. **D89**, 094508 (2014), arXiv:1402.6656 [hep-lat].
[15] W. Detmold, M. McCullough, and A. Pochinsky, Phys.Rev. **D90**, 115013 (2014), arXiv:1406.2276 [hep-ph].
[16] W. Detmold, M. McCullough, and A. Pochinsky, Phys.Rev. **D90**, 114506 (2014), arXiv:1406.4116 [hep-lat].
[17] Z. Fodor, K. Holland, J. Kuti, S. Mondal, D. Nogradi, *et al.*, (2015), arXiv:1501.06607 [hep-lat].
[18] R. S. Chivukula, A. G. Cohen, M. E. Luke, and M. J. Savage, Phys.Lett. **B298**, 380 (1993), arXiv:hep-ph/9210274 [hep-ph].
[19] J. Bagnasco, M. Dine, and S. D. Thomas, Phys.Lett. **B320**, 99 (1994), arXiv:hep-ph/9310290 [hep-ph].
[20] M. Pospelov and T. ter Veldhuis, Phys.Lett. **B480**, 181 (2000), arXiv:hep-ph/0003010 [hep-ph].
[21] G. D. Kribs, T. S. Roy, J. Terning, and K. M. Zurek, Phys. Rev. **D81**, 095001 (2010), arXiv:0909.2034 [hep-ph].
[22] M. R. Buckley and E. T. Neil, Phys.Rev. **D87**, 043510 (2013), arXiv:1209.6054 [hep-ph].
[23] T. Appelquist, R. C. Brower, M. I. Buchoff, G. T. Fleming, X.-Y. Jin, J. Kiskis, G. D. Kribs, E. T. Neil, J. C. Osborn, C. Rebbi, E. Rinaldi, D. Schaich, C. Schroeder, S. Syritsyn, P. Vranas, E. Weinberg, and O. Witzel (Lattice Strong Dynamics (LSD) Collaboration), (2015), arXiv:1503.04203 [hep-ph].
[24] M. E. Luke, A. V. Manohar, and M. J. Savage, Phys.Lett. **B288**, 355 (1992), arXiv:hep-ph/9204219 [hep-ph].
[25] A. L. Fitzpatrick, W. Haxton, E. Katz, N. Lubbers, and Y. Xu, (2012), arXiv:1211.2818 [hep-ph].
[26] A. L. Fitzpatrick, W. Haxton, E. Katz, N. Lubbers, and Y. Xu, JCAP **1302**, 004 (2013), arXiv:1203.3542 [hep-ph].
[27] R. J. Hill and M. P. Solon, (2014), arXiv:1401.3339 [hep-ph].
[28] R. J. Hill and M. P. Solon, (2014), arXiv:1409.8290 [hep-ph].
[29] M. T. Frandsen, U. Haisch, F. Kahlhoefer, P. Mertsch, and K. Schmidt-Hoberg, JCAP **1210**, 033 (2012), arXiv:1207.3971 [hep-ph].
[30] N. Weiner and I. Yavin, Phys.Rev. **D86**, 075021 (2012), arXiv:1206.2910 [hep-ph].
[31] G. Ovanesyan and L. Vecchi, (2014), arXiv:1410.0601 [hep-ph].
[32] J. Kotila and F. Iachello, Phys.Rev. **C85**, 034316 (2012), arXiv:1209.5722 [nucl-th].
[33] M. Mustonen and J. Engel, Phys.Rev. **C87**, 064302 (2013), arXiv:1301.6997 [nucl-th].
[34] W. Detmold, B. C. Tiburzi, and A. Walker-Loud, Phys.Rev. **D79**, 094505 (2009), arXiv:0904.1586 [hep-lat].
[35] W. Detmold, B. Tiburzi, and A. Walker-Loud, Phys.Rev. **D81**, 054502 (2010), arXiv:1001.1131 [hep-lat].
[36] R. G. Edwards and B. Joo (SciDAC), Nucl. Phys. Proc. Suppl. **140**, 832 (2005), arXiv:hep-lat/0409003.
[37] G. S. Bali and F. Bursa, JHEP **0809**, 110 (2008), arXiv:0806.2278 [hep-lat].
[38] G. Colangelo, S. Durr, A. Juttner, L. Lellouch, H. Leutwyler, *et al.*, Eur.Phys.J. **C71**, 1695 (2011), arXiv:1011.4408 [hep-lat].
[39] K. Olive *et al.* (Particle Data Group), Chin.Phys. **C38**, 090001 (2014).
[40] J. Billard, L. Strigari, and E. Figueroa-Feliciano, Phys.Rev. **D89**, 023524 (2014), arXiv:1307.5458 [hep-ph].
[41] K. M. Zurek, Phys.Rept. **537**, 91 (2014), arXiv:1308.0338 [hep-ph].
[42] S. D. McDermott, H.-B. Yu, and K. M. Zurek, Phys.Rev. **D85**, 023519 (2012), arXiv:1103.5472 [hep-ph].
[43] J. Bramante, K. Fukushima, and J. Kumar, Phys.Rev. **D87**, 055012 (2013), arXiv:1301.0036 [hep-ph].
[44] B. Bertoni, A. E. Nelson, and S. Reddy, Phys.Rev. **D88**, 123505 (2013), arXiv:1309.1721 [hep-ph].